Petroleum Science 23 (2026) 897–912

Contents lists available at ScienceDirect

Petroleum Science

journal homepage: www.keaipublishing.com/en/journals/petroleum-science

Original Paper

Study of the effect of nanoemulsion on the EOR in low-permeability, highly waxy oil reservoirs based on NMR displacement experiments

Rui-Jie Fei [a,b], Ming-Hui Li [c,*], Shuai Yuan [a,b], Chen Cao [c], Fu-Jian Zhou [a,b,**], Er-Dong Yao [a,b], Hao Bai [a,b], Diu-Wei Ding [a,b]

[a] State Key Laboratory of Petroleum Resources and Engineering, China University of Petroleum (Beijing), Beijing, 102249, China
[b] Unconventional Petroleum Research Institute, China University of Petroleum (Beijing), Beijing, 102249, China
[c] Oil & Gas and New Energy Branch, PetroChina Corporation, Beijing, 100010, China

ARTICLE INFO

Article history:
Received 9 November 2024
Received in revised form
3 November 2025
Accepted 5 November 2025
Available online 13 November 2025

Edited by Yan-Hua Sun

Keywords:
EOR of highly waxy oil reservoir
Wax deposition damage
Nanoemulsion
NMR

ABSTRACT

Wax precipitation damage caused by cold water injection or temperature reduction is very commonly seen in the development of waxy crude oil reservoirs. Various methods for eliminating wax precipitation damage have been studied by many scholars, such as injecting hot water, artificial fracture, and using chemical dewaxing agents. However, the effects of nanoemulsion on wax crystals and enhanced oil recovery (EOR) have not yet been systematically studied. This study used core displacement system based on nuclear magnetic resonance (NMR) to investigate the effect of nanoemulsion on the EOR in low-permeability, waxy oil reservoirs. Some influencing factors such as injection water temperatures, core permeability, fractured/unfractured core, and nanoemulsion concentration conditions have been investigated. Meanwhile, the wax crystal morphology and quantity have been studied before and after using nanoemulsion using a polarizing microscope. The main conclusions are as follows: (1) After injecting 60 °C hot water, the recovery can be increased from 19.36% to 32.82%, which can alleviate wax deposition damage to a certain extent. (2) Enhancing core permeability or using fractured cores can increase the flow capacity of displacement fluid within the core and enhance waxy crude oil recovery. The EOR after improving core permeability is 10.22%, while the EOR of the fractured core is 26.24%. (3) Nanoemulsions can dissolve wax crystals in waxy crude oil and inhibit their formation to achieve EOR. The crude oil recovery at nanoemulsion concentrations of 0.1, 0.5, and 1.0 wt% were 34.84%, 38.24%, and 42.85%, respectively. (4) The use of nanoemulsion can reduce the number, area ratio, and fractal dimension of wax crystals, thereby mitigating wax deposition damage. Using a 1 wt% of nanoemulsion, the area ratio of wax crystals decreased from 47.25% to 16.67%, and the number of wax crystals decreased from 1309 to 496.

1. Introduction

Waxy oil reservoirs are abundant and widely distributed in Northeast China, Xinjiang, Central Asia, Northern Europe, and North America around the world (Burger et al., 1981; Chen et al., 2017; Ding et al., 2006; Kiyingi et al., 2022). Waxy crude oil contains a high amount of long-chain paraffin wax compounds, which makes the crude oil have a high pour point, low density, and variable viscosity with temperature (Li B. et al., 2024; Temizel et al., 2018). When developing highly waxy oil reservoirs, it is important to consider the wax deposition damage due to the decrease in formation temperature, which will cause the reduction in reservoir porosity and effective permeability, changes in crude oil composition and rheological properties (El-Dalatony et al., 2019; Wang et al., 2019; Yang et al., 2013). However, in actual oilfield production, the phenomenon of formation temperature decrease is very common because large amounts of cold working fluids are injected into the formation while oil well production stimulation measures or water injection development are implemented (Nie and Yang, 2014). In this situation, frequent wax deposition will

* Corresponding author.
** Corresponding author.
E-mail addresses: lmhcupb@163.com (M.-H. Li), zhoufj@cup.edu.cn (F.-J. Zhou).
Peer review under the responsibility of China University of Petroleum (Beijing).

https://doi.org/10.1016/j.petsci.2025.11.013

occur not only in the wellbore but also in the formation, which will further affect normal oil well production and reservoir recovery (El-Dalatony et al., 2019).

Up to now, numerous scholars have studied the factors affecting wax deposition, wax crystal morphology characteristics, and the impact of wax deposition on the properties of crude oil by establishing various wax deposition models and carrying out laboratory experiments (Li M. et al., 2024; Yang et al., 2020; Zhang et al., 2025). Huang et al. (2011) investigated the effect of operating temperature on wax deposition using the Michigan Wax Predictor (MWP) model. They found that when the oil temperature rose from 15.3 to 35.4 °C, the characteristic mass J_{wax} of wax deposition decreased from 36.17 to 23.57 wt%. Zhao et al. (2022) used a microscope to quantitatively characterize the relationship between the rheological rate of waxy crude oil and the number of wax crystals. It was found that as the rheological rate increased from 0.5 to 10 s^{-1}, the number of wax crystals decreased by 89%. At the same time, they also observed that as the shear stress increased, the waxy crude oil would undergo destruction of the wax crystal and crude oil flocculation structure (Zhao et al., 2024). Vieira et al. (2010) studied the effect of pressure on wax precipitation in crude oil using high-pressure microcalorimetry. They found that increasing pressure significantly affects wax appearance temperature (WAT) and crystallization enthalpy. When the pressure was increased from 1.01 to 200 bar, the WAT rose from 44.6 to 46.5 °C (Vieira et al., 2010). Kasumu et al. (2013) used a modified visual method to find that the WAT value is not fixed, but shows a linear relationship that decreases as the cooling rate increases. Wang et al. (2023) also found that rapid cooling rates (> 300 °C/min) of crude oil result in the formation of dense needle-shaped crystals, while slow cooling rates (1–3 °C/min) result in the formation of spherulitic crystals. Kané et al. (2004) observed that under static conditions, as the temperature of waxy crude oil decreases, wax crystals gradually grow laterally and accumulate to form larger aggregates and complex network structures, which significantly increase the viscosity of crude oil, and Yalaoui et al. (2020) also found that when crude oil temperature drops below the WAT, wax crystals precipitate in a lamellar form, and these crystals gradually aggregate and restrict the liquid oil phase in nanoscale gaps. Consequently, viscosity increased and fluidity deteriorated (Yalaoui et al., 2020).

The precipitation of wax crystals not only affects the composition and properties of crude oil, but also causes wax deposition damage during oilfield development, affecting the development results. In response to the wax deposition damage caused by differences in the environment of waxy reservoirs and the different ways of changing reservoir conditions, many scholars have proposed different stimulation methods, such as hot water injection, fracturing, and chemical wax removal agent injection (Adebiyi, 2020; Ali et al., 2022; Wang et al., 2021). Xie et al. (2020) studied the low-temperature damage and hot water injection improvement in the highly waxy oil reservoir of Changchunling. They pointed out that wax precipitation mainly occurs within 15 m of the wellbore, and when the injection-water temperature is higher than WAT, the relative permeability of crude oil increases by 15%–20%. This improvement is attributed to the reduction in crude oil viscosity and the prevention of wax crystallization in the reservoir pores, thereby maintaining higher porosity and permeability (Xie et al., 2020). Zhou et al. (2010) studied the effect of hot water displacement on the oil recovery of the Liaohe Oilfield through core displacement experiments. They found that due to the influence of wax deposition, the crude oil recovery decreased from 68.7% at 70 °C to 34.3% at 55 °C, and the average core permeability also decreased from 1300 to 356 mD (Zhou et al., 2010). Trushin et al. (2021) developed a methodology to determine that the minimum volume of hot water injected was 1.25 pore volumes, which would not cause a decline in oil recovery when switching to cold water injection (Trushin et al., 2021). Babadagli (2003) studied fractured waxy reservoirs and found that fluids in fractures can drive crude oil out of the core through capillary forces and other mechanisms, increasing the ultimate recovery of hot water displacement by 30% (Babadagli, 2003).

For the use of chemical inhibitors, current research for waxy oil fields mainly focuses on inhibiting wax crystallization to reduce the WAT and pour point of waxy crude oil, and inhibiting wax precipitation to improve the flowability of crude oil (Al-Shboul et al., 2023; Eke et al., 2022; Ragunathan et al., 2020). Cao J. et al. (2022) used molecular dynamics simulations to reveal the effect of pour point depressant (PPD) on the phase transition point of waxy crude oil. After adding PPD, the phase transition temperature decreased from 296.439 to 287.602 K, and the wax crystals were evenly distributed, thereby reducing the viscosity of crude oil and improving low-temperature fluidity (Cao J. et al., 2022). Xia et al. (2022) prepared a macroporous comb-like polymeric pour-point depressant (MP-POA) using a high-internal-phase-emulsion (HIPEs) template, which optimally balanced crystallization ability and nucleation template effect at 0.5 wt% cross-linker, thereby lowering the pour point of waxy oil by 3 °C (Xia et al., 2022). He et al. (2016) found that nano-hybrid pour point depressant (NPPD) can reduce the pour point and WAT of waxy crude oil by inhibiting wax crystal precipitation and inhibiting wax aggregation through electrostatic repulsion. Using 1 wt% NPPD, the crude oil pour point can be reduced from 30 to 21 °C, the WAT from 56.5 to 54.0 °C, and the wax precipitation rate from 16.5 to 15.3 wt% (He et al., 2016). Zhang et al. (2024) developed a new water-in-oil ethylene-vinyl acetate (EVA) nanoemulsion viscosity improver, which reduced the viscosity and yield stress of crude oil by 52.8% and 29.6%, respectively, compared to traditional EVA, thereby improving the fluidity of crude oil (Zhang et al., 2024). In terms of inhibition efficiency of chemical reagents, Gurgel Aum et al. (2024) found that water-in-oil microemulsions prepared using nonionic surfactants can effectively dissolve paraffin deposits, with microemulsion systems containing kerosene achieving a wax removal efficiency of up to 66.78% (Gurgel Aum et al., 2024). Towler et al. (2011) found that the use of inhibitors could reduce wax deposition by 35% at 5 °C. At 15 °C, wax deposition could be reduced by 60%. Inhibitors are more effective at higher temperatures, while higher concentrations are required at lower temperatures to achieve better inhibition effects (Towler et al., 2011). However, the internal mechanisms by which nanoemulsions improve the flowability of waxy crude oil and enhance crude oil recovery still require further study. At the same time, quantitative methods for monitoring the effects of nanoemulsions on wax crystals and EOR are still inadequate and warrant further refinement.

In view of the above summary and the shortcomings of existing research, this paper uses a core displacement device based on NMR to explore the impact of injection water temperature, core permeability, fractured/unfractured cores, and nanoemulsion concentration on EOR in waxy crude oil reservoirs. Meanwhile, using a polarizing microscope, we observed and quantitatively summarized the wax crystal precipitation phenomena and morphological characteristics of waxy crude oil at different temperatures and with or without the addition of nanoemulsions, which further deepened our understanding of wax deposition and explored the mechanism of wax inhibition. This work not only provides experimental support for mitigating wax deposition damage but also holds important practical significance for engineering applications.

2. Experimental materials and equipment

2.1. Waxy crude oil

The crude oil used is from the GeTybai Oilfield in Kazakhstan. In order to ensure that the crude oil accurately reflects the physical and chemical properties of the field and can be reused, it underwent pretreatment by heating in an inflatable environment in the laboratory (Yan and Luo, 1987). The basic physical properties of crude oil are shown in Table 1. Its density is 0.88 g/cm^3, and its viscosity at 50 °C is 23.23 mPa·s. As determined by differential scanning calorimeter (TA-Q2000), the WAT of this oil sample is 59.06 °C, with a wax content of 22.06%. According to GB/T 30431-2020 laboratory gas chromatography testing standard, the carbon number range of normal saturated hydrocarbons in the studied oil sample is n-C_5–n-C_{34} (Fig. 1), mainly light hydrocarbons (C_5–C_{13}) and medium hydrocarbons (C_{14}–C_{25}), and the content of heavy normal hydrocarbons (n-C_{26+}) is 15.73%.

2.2. Nanoemulsion system

The displacement fluids used in the experiment included deuterium water and nanoemulsion (Fig. 2). The nanoemulsion used in this study is a Winsor-IV type bicontinuous microemulsion system, formulated via a low-energy spontaneous emulsification method. Its main components include a nonionic polyoxyethylene ether as a surfactant, a low-carbon chain alcohol as a cosurfactant, a terpene-based oil core, and deionized water as the solvent. When diluted with water, this nanoemulsion forms a clear and transparent water-in-oil system with high salinity tolerance and excellent thermal stability. The viscosity of the nanoemulsion stock solution is 36.5 mPa·s, and its critical micelle concentration (CMC) is 0.015 wt%. At room temperature, its surface tension is 25.0 mN/m, and the peak droplet size of the 0.1 wt% nanoemulsion is 10.01 nm.

2.3. Experimental core samples

The cores used in this experiment were taken from the J_8 and J_{12} layers of the GeTybai Oilfield (Fig. 3). The average permeability of the former layer is approximately 20 mD, while that of the latter layer is approximately 200 mD. All cores are sandstone cores that have been processed into standard cores with a diameter of 25 mm and a length of 50 mm. Table 2 lists the basic physical properties of all cores. Cores #1, #2, #7–#9 are 20 mD low-permeability cores, cores #3 and #4 are 200 mD high-permeability cores, and cores #5 and #6 are 20 mD fractured cores. The fracture in core #6 completely penetrates the core in the longitudinal direction, while the fracture in core #5 penetrates half of the core in the longitudinal direction.

2.4. Analysis of wax precipitation by polarizing microscope and differential scanning calorimeter

The variations in wax crystal morphology and quantity can be intuitively analyzed using a BX53M polarizing microscope and ImageJ software (Fig. 4). It has a 20*20 magnification and is paired with a Linkam PE60 liquid nitrogen temperature stage for precise temperature control (±0.1 °C). A ColSNAP 3.3M digital camera was used for high-resolution imaging of wax crystal morphology and quantity. During wax crystal image processing, images taken by the microscope were sharpened and enhanced in clarity and resolution using tools like Adobe Premiere. Then, the image recognition and wax crystal quantitative statistics can be completed using the steps of color-gray image conversion, threshold segmentation, and contour recognition-numerical statistics in ImageJ software. This included 8-bit image processing to convert color to grayscale. By setting parameters like particle size and circularity based on actual wax crystal features, valid wax crystal contours

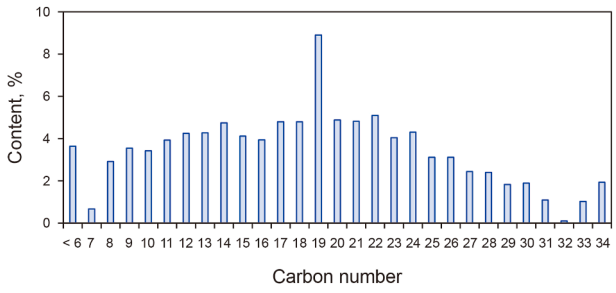

Fig. 1. Carbon number distribution of normal saturated hydrocarbons in the experimental crude oil.

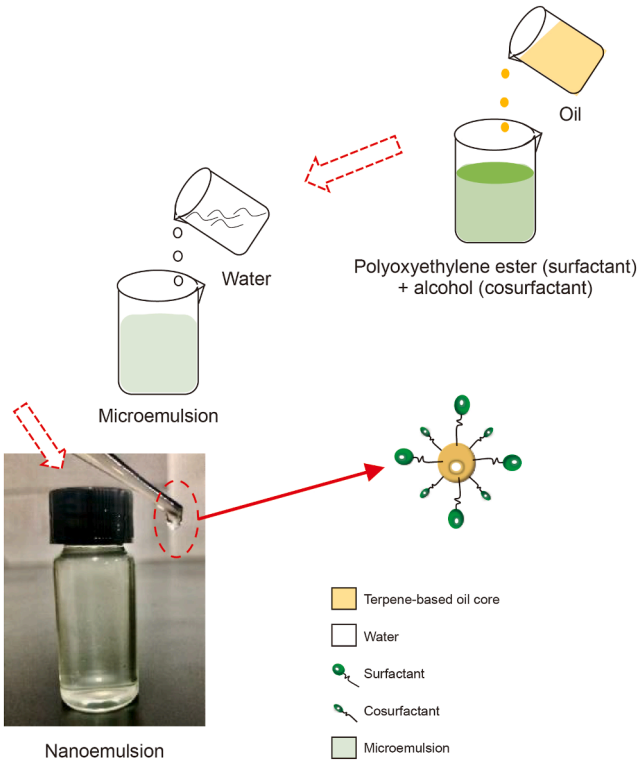

Fig. 2. Nanoemulsion system.

Table 1
Basic physical properties of waxy crude oil.

Density at 20 °C, g/cm^3	Viscosity at 50 °C, mPa·s	WAT, °C	Wax content, %	Saturates, wt%	Aromatics, wt%	Resins, wt%	Asphaltenes, wt%	Others, wt%	Total yield, %
0.88	23.23	59.06	22.06	56.31	8.74	14.50	1.30	19.15	80.85

(a) 20 mD cores **(b)** 200 mD cores **(c)** Fractured cores

Fig. 3. Experimental cores.

Table 2
Basic parameters of experimental cores.

Core No.	Diameter, cm	Length, cm	Porosity, %	Permeability, mD
#1	2.58	4.98	17.77	21.58
#2	2.61	4.95	17.92	19.35
#3	2.50	4.97	18.06	200.70
#4	2.52	4.93	17.94	201.30
#5	2.49	5.02	16.60	21.30
#6	2.56	5.12	18.12	20.13
#7	2.51	4.60	16.60	19.85
#8	2.54	4.97	18.76	20.21
#9	2.69	4.98	16.11	20.56

were selected. Finally, the "Analyze Particles" function was used to extract and count parameters like wax crystal quantity and wax precipitation area (Zhao J. et al., 2023).

The wax precipitation of oil samples was tested using a differential scanning calorimeter (DSC) (TA-Q2000) (Fig. 4) per the Industry Standard SY/T0545-2012, and the curve of heat flux with temperature was drawn to determine the WAT and wax content of crude oil. The air without phase change and with a small heat capacity change was used as the control sample. The thermal monitoring system records the thermal flow difference of the sample at different temperatures, generating a DSC curve to study the wax precipitation process.

2.5. Core displacement system based on nuclear magnetic resonance

As shown in Fig. 5, the core displacement system based on NMR included an NMR monitoring device, a constant temperature and pressure displacement pump, a thermal insulation intermediate container, a core holder, and a thermal insulation pipeline. The initial displacement fluid was placed in an insulated intermediate container (Fig. 5(b)), and then pumped into the core holder through the constant temperature and pressure displacement pump of Fig. 5(a). The NMR monitoring device used a MacroMR12-150H-I nuclear magnetic resonance spectrometer (NIUMAG, Shanghai, China) (Fig. 5(d)) to measure changes in oil and water distribution and recovery during oil flooding. T_2 was measured using the Carr-Purcell-Meiboom-Gill (CPMG) sequence. The specific NMR parameters are shown in Table 3.

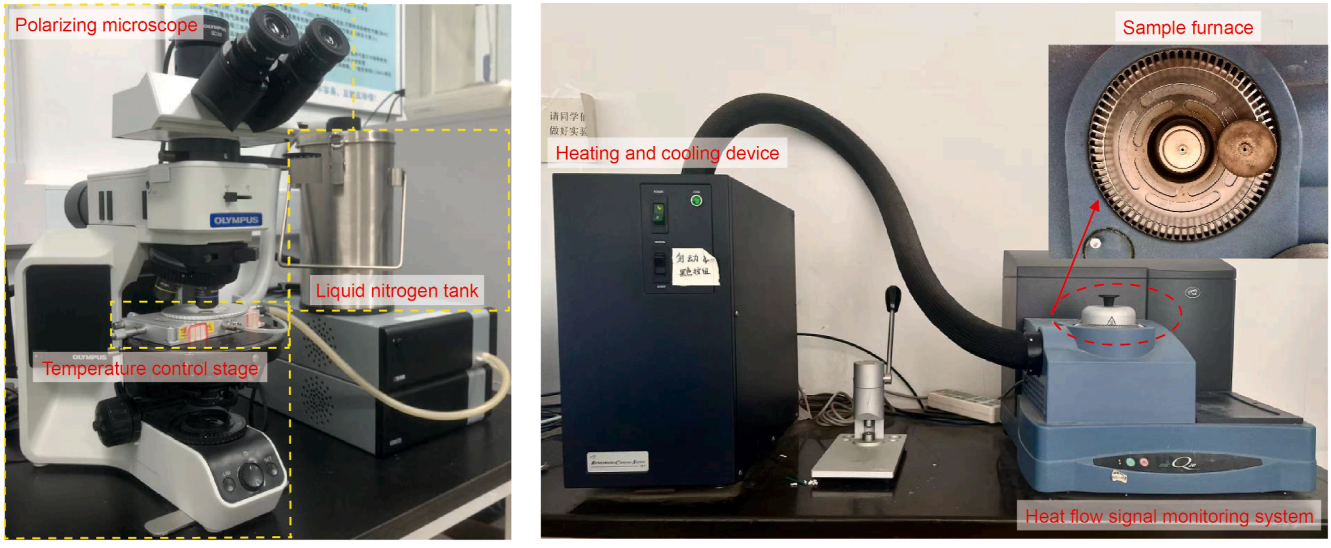

(a) Polarizing microscope **(b)** Differential scanning calorimeter

Fig. 4. Polarizing microscope and differential scanning calorimeter.

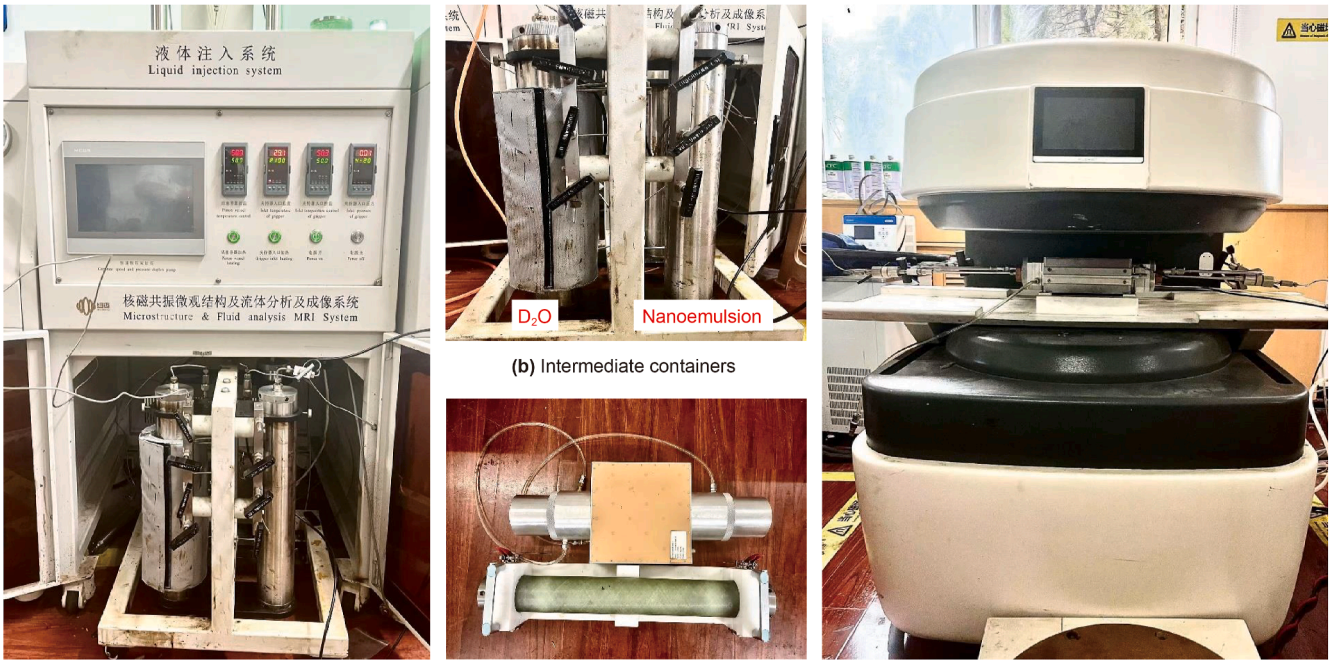

(a) Displacement pump (b) Intermediate containers (c) Core holder (d) NMR monitoring device

Fig. 5. Core displacement system based on nuclear magnetic resonance.

Table 3
The measurement parameters of T_2 spectra.

Field frequency, MHz	Magnetic field intensity, T	Polarization time, ms	Echo spacing, ms	Echo number	Scanning times
12.448	0.3	3000	0.2	18000	16

3. Experimental scheme and process

3.1. Observation of wax crystal morphology and quantitative characterization

Four sets of experiments were designed for polarizing microscopy observation and differential scanning calorimetry testing to observe changes in wax crystal morphology and quantity before and after the addition of nanoemulsion to crude oil, as well as changes in WAT and wax precipitation in crude oil. The experimental procedures are as follows:

(1) Divide the pretreated crude oil into four groups. Add nanoemulsion of different concentrations (0, 0.1, 0.5, and 1.0 wt%) to each group.
(2) Place 0.5–1.0 g of oil sample on a polarizing microscope slide, heat at a rate of 5 °C/min to 80 °C, and let stand for 20 min.
(3) Using a liquid nitrogen temperature console stage, cool the oil samples at a rate of 0.5 °C/min while keeping the camera running to record video of the samples from 80 to 30 °C to avoid delays caused by untimely capture of a single picture. Randomly select three different fields of view in each sample for observation to ensure representativeness.
(4) Observe the nucleation and crystallization process of wax in the four groups of oil samples. The temperature at which the wax crystal particle size exceeds 1 μm is denoted as WAT (Wang et al., 2020).
(5) Select photos from the oil sample video without nanoemulsion at temperatures of 50, 40, and 30 °C, and select photos from the oil sample video with nanoemulsion at 30 °C. After processing all photos using Adobe Premiere, use ImageJ software for quantitative statistical analysis of wax crystal parameters.
(6) Place the four groups of waxy crude oil samples and air samples in the differential scanning calorimetry sample furnace in order, heat to 80 °C, and cool at a constant gradient of 0.1 °C/min.
(7) The temperature at which the heat flow curve deviates from the baseline for the first time due to the heat release during the wax precipitation process is the wax WAT of the crude oil.
(8) The heat released and the mass of the substance in the range from the wax WAT to −20 °C are determined. The cumulative heat release of wax deposition is calculated by integrating the curve. Using 210 J/g as the crystallization heat of wax, the cumulative wax deposition amount of the oil sample is determined by the ratio of these two values.

3.2. Analysis of waxy crude oil recovery under different displacement conditions

3.2.1. Experimental scheme

Nine groups of core displacement tests based on NMR were designed to study the effects of injection water temperature (cores #1 and #2), core permeability (cores #3 and #4), fractured/unfractured core (cores #5 and #6), and nanoemulsion concentrations (cores #7–#9) on the recovery of waxy crude oil (Table 4). At the same time, the displacement velocity of the displacement

Table 4
Different core displacement experiments.

Test core No.	Permeability, mD	Test variables	Displacement temperature, °C	Displacement fluid
#1	21.58	Displacement fluid temperature	30	Deuterium water
#2	19.35		60	
#3	200.70	Core permeability	30	
#4	201.30		60	
#5	21.30	Fracture length	30	
#6	20.13		30	
#7	19.85	Nanoemulsion concentration	30	0.1 wt% nanoemulsion
#8	20.21		30	0.5 wt% nanoemulsion
#9	20.56		30	1.0 wt% nanoemulsion

fluid was selected as 0.1 mL/min, and the confining pressure was 8 MPa.

3.2.2. Experimental process

The main steps of the core displacement experiment are as follows:

Step 1: Experimental cores were dried at 90 °C, weighed, and allowed to stand in a vacuum device for one day.
Step 2: Dry cores and preprocessed crude oil were placed in a medium container. The cores were saturated at 80 °C and 12 MPa for a week, then the saturated core weight was recorded to calculate saturation.
Step 3: The NMR equipment was calibrated, and the appropriate coil and CPMG sequence were selected to ensure a strong correlation between the NMR signal intensity and the crude oil saturation in the cores (Sun et al., 2024).
Step 4: Install saturated core #1 in the core holder, set the temperature of the core holder to 30 °C, and maintain the water at 30 °C for displacement.
Step 5: After the core #1 displacement was completed, the displacement measurements of cores #2–#9 were completed in turn. For cores #2 and #4, the displacement fluid temperature was adjusted to 60 °C; for cores #7–#9, the displacement fluid was a nanoemulsion with different concentrations (0.1, 0.5, and 1.0 wt%), and the rest was the same as Step 4.

4. Experimental results and analysis

4.1. The effect of nanoemulsion on wax crystal in waxy crude oil

4.1.1. The change of wax crystal morphology and quantity

As shown in Fig. 6(a), with a lower temperature, wax crystals initially precipitate as individual particles, which subsequently aggregate to form wax crystal aggregates. With further cooling, these aggregates undergo compression, ultimately forming a stable three-dimensional waxy gel structure (Zhao et al., 2022, 2024). At 30 °C, under complete wax deposition conditions, the waxy gel structure exhibits a contiguous, flocculated, and dispersed morphology. The wax crystal aggregates are highly irregular and randomly distributed within the observation field. Their morphology is diverse, with varying sizes and structural complexity. In this state, the crude oil exhibits high viscosity and poor fluidity with wax deposition damage due to the effects of wax precipitation and waxy gel structure (Li B. et al., 2024).

With the addition of nanoemulsion, the flocculated structures gradually disappear, and the wax crystal aggregates break down into more orderly structures, as shown in Fig. 6(d)–(f). As the nanoemulsion concentration further increases, wax crystals cease to interconnect and instead form independent aggregates of varying sizes and morphology. This transformation is the fundamental mechanism by which nanoemulsion inhibits wax deposition and improves the rheological behavior of waxy crude oil (Benavides et al., 2020).

As shown in Fig. 7, the quantitative analysis of wax deposition characteristics of crude oil (without nanoemulsion) reveals that with a decrease in temperature, the wax precipitation area, average aspect ratio, and boundary box fractal dimension significantly increase. This indicates that the morphology of wax crystals becomes increasingly complex, leading to a stronger gel structure in crude oil. However, despite the increase in the wax precipitation area, the overall number of wax crystals decreases. This phenomenon arises because, as the temperature further decreases, the position of wax crystal aggregates stabilizes, and smaller aggregates continue to grow and coalesce into larger ones, resulting in an overall reduction in the number of individual wax crystals. As shown in Fig. 7, with the introduction of the nanoemulsion and increasing concentration, the number of wax crystals, wax precipitation area, average aspect ratio, and boundary box fractal dimension all decrease. For instance, when a 1.0 wt% nanoemulsion is added to crude oil, the number of wax crystals and the wax precipitation area decrease by a factor of three, while the average aspect ratio and boundary box fractal dimension also exhibit a significant reduction. These findings demonstrate that nanoemulsion effectively inhibits wax crystal precipitation and aggregation, thereby mitigating flocculation and deposition damage in waxy crude oil (Dong et al., 2020).

4.1.2. The change of wax appearance temperature

The WAT of the four oil samples observed using a polarizing microscope is shown in Fig. 8. In the absence of nanoemulsion, fine wax crystals begin to precipitate at 61 °C within the observation field. However, with the addition of nanoemulsion, WAT progressively decreases, reaching 57 °C at a nanoemulsion concentration of 1.0 wt%. This result suggests that nanoemulsion effectively inhibits the precipitation of new wax crystals, thereby lowering the WAT of crude oil. However, the WAT measured here without adding nanoemulsion is slightly higher than the value measured by DSC in Table 1. This is because the microscopic observation method only needs to observe one or more wax crystal particles, while the DSC method usually needs to precipitate a certain number of wax crystal particles to be detected, so the temperature is slightly lower (Cao L. et al., 2022; Japper-Jaafar et al., 2016).

The precipitation, aggregation, and flocculation of wax crystals have a highly complex impact on the physicochemical properties of waxy crude oil. Analysis of changes in wax crystal morphology and quantity before and after adding nanoemulsion indicates that nanoemulsions exhibit a significant inhibitory effect on the precipitation and aggregation of wax crystals in waxy crude oil. To further validate this process, DSC measurements were conducted (Fig. 9). As the temperature decreases, the wax crystal precipitates and releases heat, and the temperature at which the heat flow

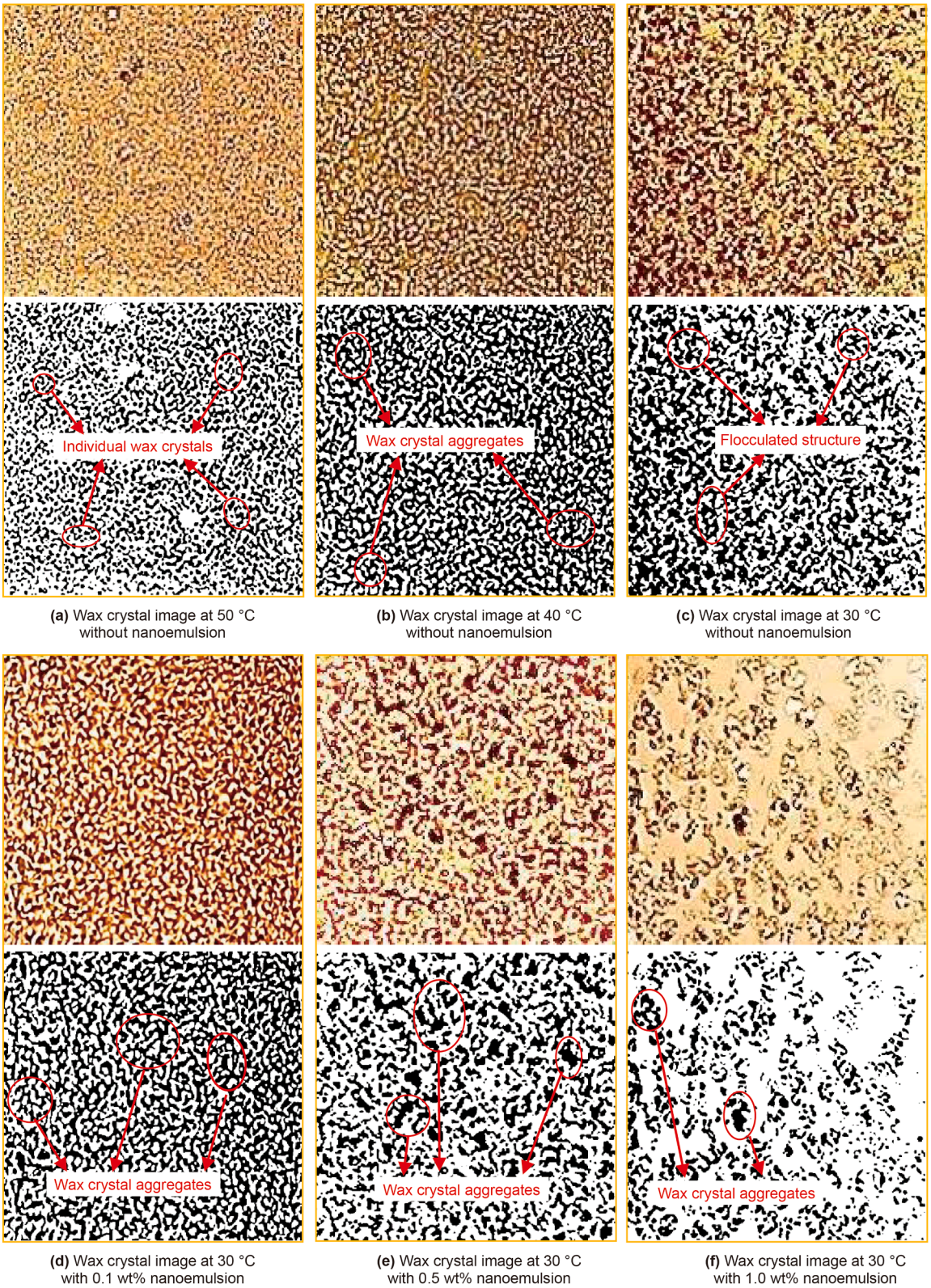

(a) Wax crystal image at 50 °C without nanoemulsion

(b) Wax crystal image at 40 °C without nanoemulsion

(c) Wax crystal image at 30 °C without nanoemulsion

(d) Wax crystal image at 30 °C with 0.1 wt% nanoemulsion

(e) Wax crystal image at 30 °C with 0.5 wt% nanoemulsion

(f) Wax crystal image at 30 °C with 1.0 wt% nanoemulsion

Fig. 6. The morphology of wax crystals in crude oil samples before and after the addition of nanoemulsion.

curve shifts is the WAT of crude oil. Similarly, we can find that nanoemulsion significantly influences the wax crystal precipitation process. With the addition of nanoemulsion, both the WAT and wax content decrease to varying extents. Under initial conditions, the WAT of the crude oil was 59.06 °C. After adding 1.0 wt% nanoemulsion, the WAT decreased to 54.74 °C. The reduction in wax content was even more pronounced, decreasing from 22% to 10.61% with the addition of 1.0 wt% nanoemulsion.

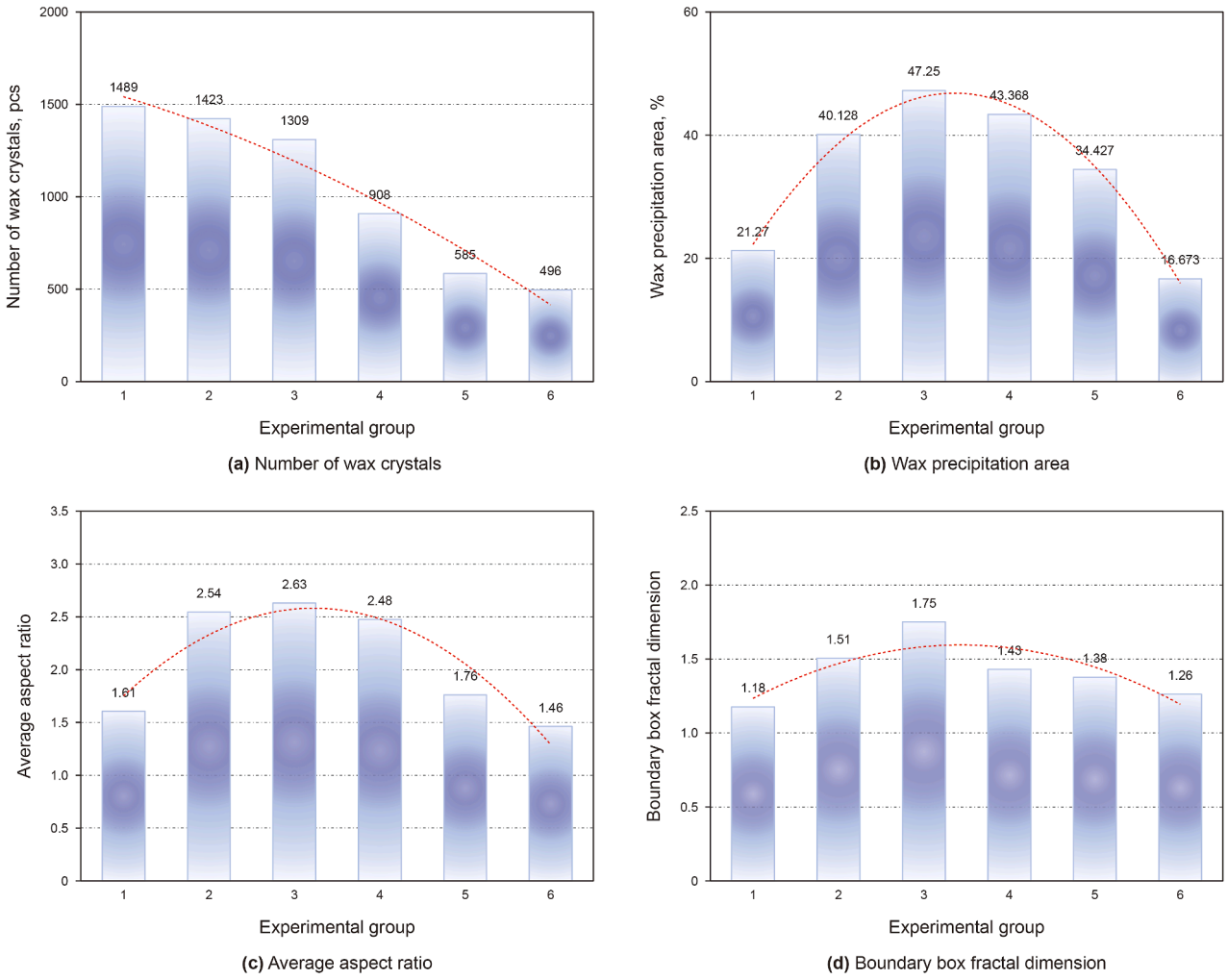

Fig. 7. Quantitative results of wax crystals in crude oil samples before (experimental groups 1–3) and after (experimental groups 4–6) the addition of nanoemulsion. In experimental groups 1–3, *w*(nanoemulsion) = 0, the experimental temperatures were 50, 40, and 30 °C, respectively; in experimental groups 4–6, the experimental temperature was 30 °C, and the nanoemulsion concentrations were 0.1, 0.5, and 1.0 wt%, respectively.

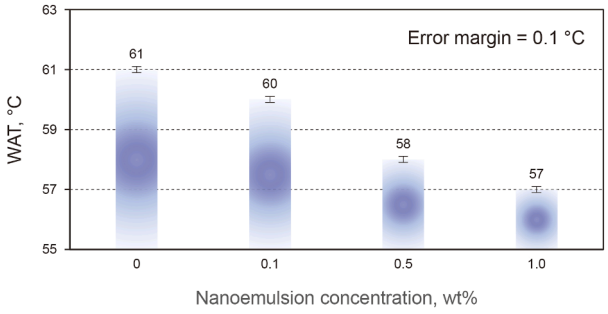

Fig. 8. WAT of crude oil samples with the addition of nanoemulsions of different concentrations.

These findings demonstrate that nanoemulsions mitigate wax deposition damage by inhibiting wax crystal precipitation and dissolving partially precipitated wax crystals, providing a basis for the subsequent discussion on the enhancement of crude oil recovery by nanoemulsions.

4.2. Analysis based on results from NMR core displacement experiments

4.2.1. The influence of water displacement temperature

By analyzing the change of T_2 spectrum collected during the displacement process, we can monitor the distribution of saturated fluids within the core in real time and quantitatively calculate the mass change of the fluids displaced within the core (Benavides et al., 2020; Elsayed et al., 2022; Zhang et al., 2023). Based on the previous research results and the T_2 spectral characteristics of the samples in this experiment, the T_2 relaxation time greater than 10 ms is considered to be the macropores, and the T_2 relaxation time of the micropores is less than 10 ms (Elsayed et al., 2022). From the polarizing microscopy test, it can be seen that the wax crystals in the crude oil varied greatly at different temperatures, which was further investigated using the NMR core displacement device, and Fig. 10 shows the T_2 spectra of cores #1 and #2 displaced at 30 and 60 °C, respectively.

The effective degree of displacement is reflected by scanning the T_2 spectrum of the displacement fluid injected with different

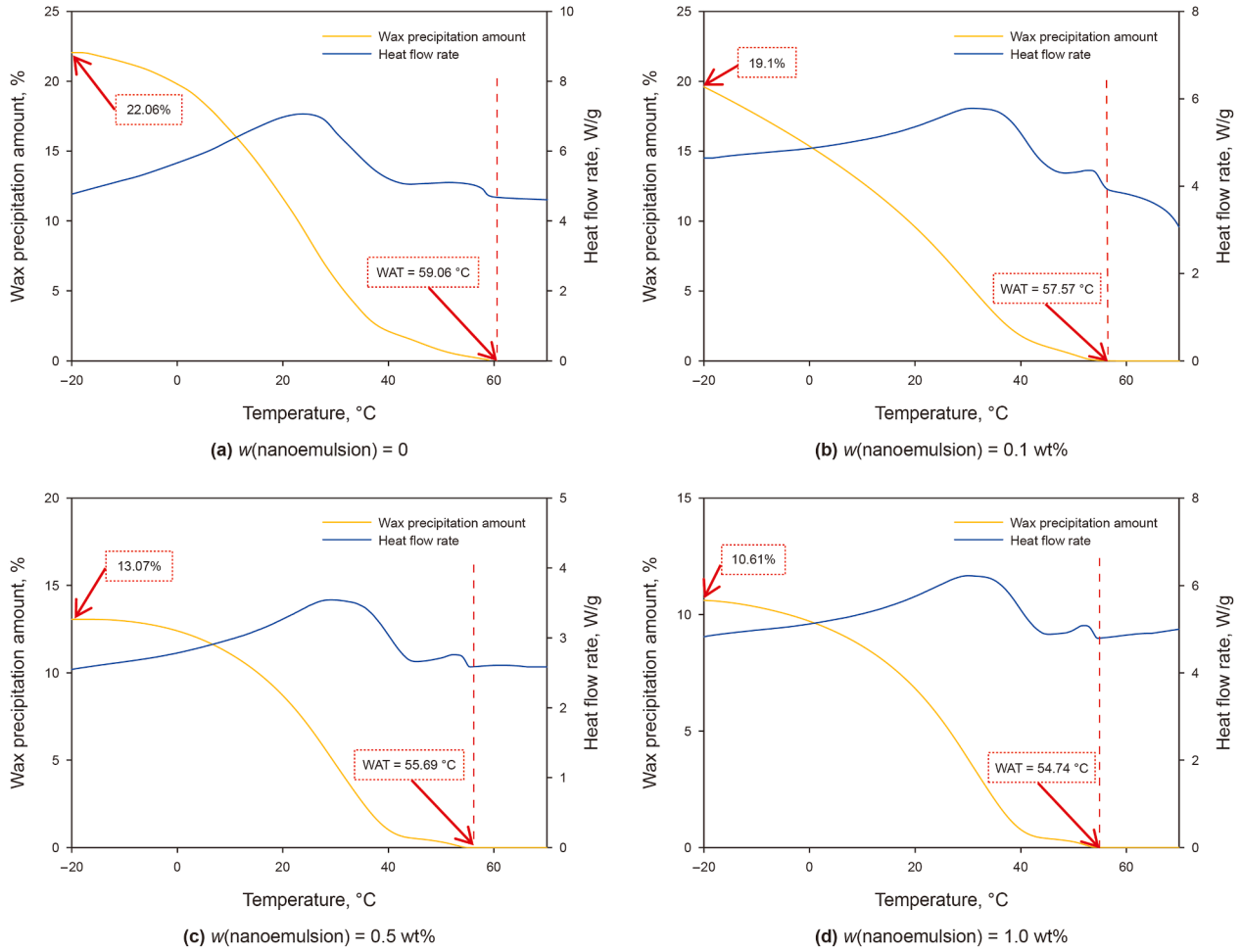

Fig. 9. DSC curves of crude oil samples with the addition of different concentrations of nanoemulsions.

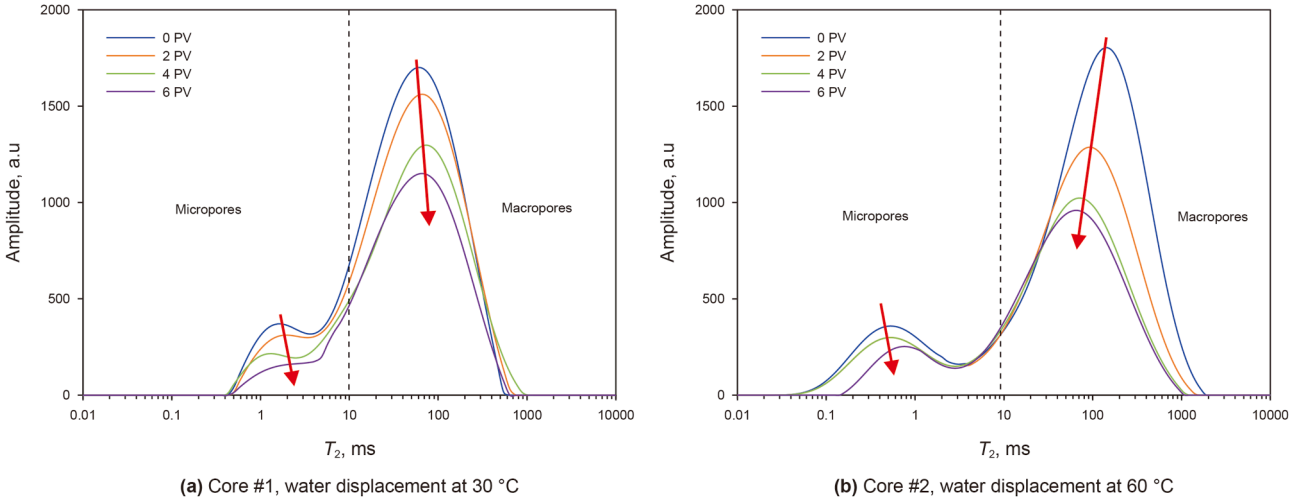

Fig. 10. T_2 spectra of 20 mD cores at different temperatures.

pore volumes (PV), where 0 PV corresponds to the saturated oil state of the core. As shown in Fig. 10, saturated crude oil is mainly concentrated in the macropores. In the process of water displacement, the change of the T_2 spectrum also mainly occurs in the macropore range. The T_2 spectrum decreases differently when different injection volume of water is injected at different temperatures. The core #1 is injected with 2 PV of water, the T_2 spectrum only decreases slightly at the macropore peak, and the spectral area does not change significantly. It takes 6 PV of water to complete the displacement. The core #2 is injected with 2 PV of

water, the spectral area and macropore peak value are significantly reduced, and displacement is basically completed when 4 PV of water is injected. Therefore, under low temperature conditions, due to the influence of wax deposition in crude oil, displacement is relatively difficult, and the area and peak value of the T_2 spectrum change are limited. When the displacement fluid temperature rises above WAT, it can effectively improve wax deposition damage in the core pores, and the displacement can be completed by injecting less displacement fluid, but the displacement is primarily of the crude oil within the macropores.

4.2.2. The influence of core permeability and fracture

Under wax deposition conditions, the increase in crude oil viscosity and the deterioration of rheological properties hinder the effective and rapid passage of displacement agents through the rock pore space. This is an important challenge faced by all highly waxy oilfields (Macary et al., 2018). This paper uses high permeability cores (cores #3 and #4) and fractured cores (cores #5 and #6) to study the effect of permeability and fracture on displacement efficiency when crude oil is in a wax deposition state.

From Fig. 11(a) and (b), after the overall permeability of the core was improved, crude oil could enter the micropores of the core, and the high-permeability core is fully saturated. Compared with the low-permeability cores (cores #1 and #2), after injecting 6 PV of water, the crude oil in the pores of the high-permeability cores is fully displaced, and the peaks and areas of micropores and macropores decreased significantly. Therefore, improving the seepage capacity of the core displacement fluid is an effective means to improve crude oil production from low-permeability reservoirs. However, at the marked position of the circle in Fig. 11(b), the position of the spectra shifts and extends outward, respectively. According to the actual porosity and permeability conditions of the core, the high-permeability core has a high seepage capacity to ensure that the crude oil inside the core can be quickly displaced. This process makes the core pores contact with water as much as possible, and a large number of fine components retained inside the pores of the core are displaced to the outside of the core, resulting in the expansion of the pore size range (Sun et al., 2023).

Due to the existence of fractures in the cores (cores #5 and #6), crude oil can enter the core pores more conveniently during the saturation process, crude oil saturation is higher than that of low-permeability cores, and the larger the fracture, the more saturated it is. The presence of favorable flow channels (fractures) increases the contact area between water and the core, which facilitates the entry of water into the core and displaces the crude oil in the pores, promoting the displacement efficiency. The displacement process involves water initially displacing oil in the fracture before

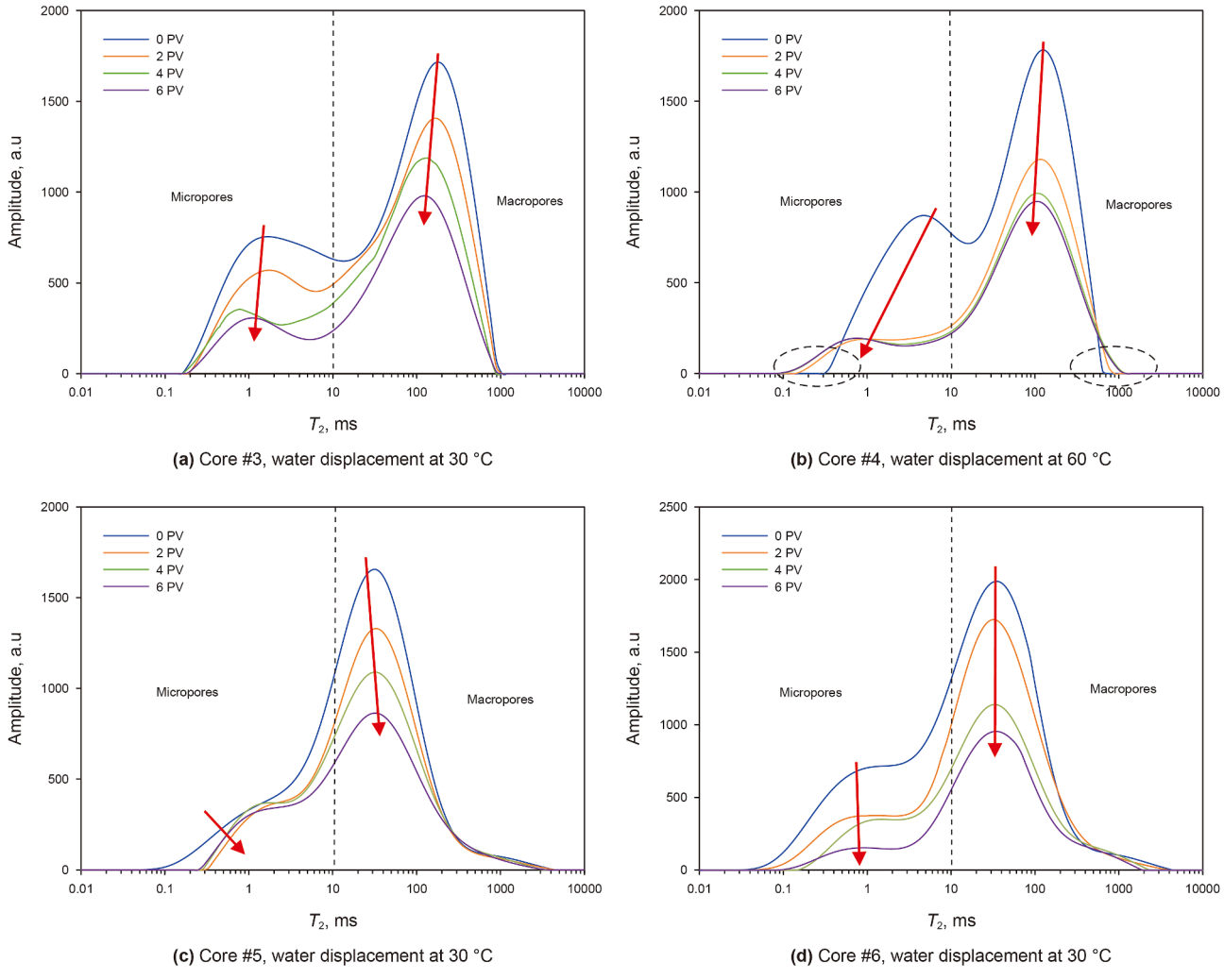

(a) Core #3, water displacement at 30 °C

(b) Core #4, water displacement at 60 °C

(c) Core #5, water displacement at 30 °C

(d) Core #6, water displacement at 30 °C

Fig. 11. T_2 spectra of cores with different permeability and fractures.

moving into the matrix area due to displacement pressure, thereby driving crude oil out of the pores (Sun et al., 2024).

4.2.3. The influence of nanoemulsion concentration

As shown in Fig. 12, the addition of nanoemulsion leads to a significant decline in the T_2 spectra of the macropore region.

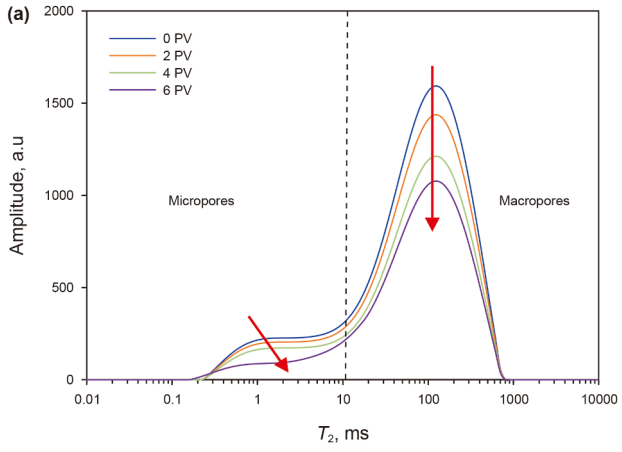

(a) Core #7, 0.1 wt% nanoemulsion displacement at 30 °C

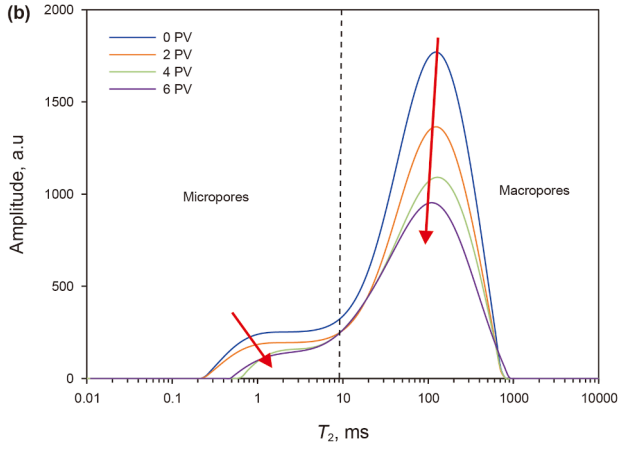

(b) Core #8, 0.5 wt% nanoemulsion displacement at 30 °C

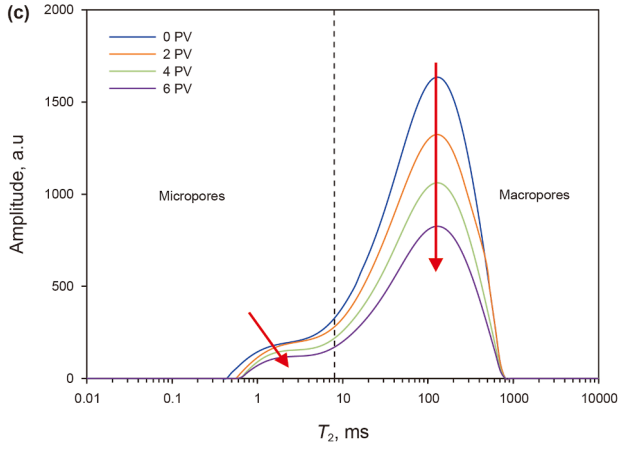

(c) Core #9, 1.0 wt% nanoemulsion displacement at 30 °C

Fig. 12. T_2 spectra of 20 mD cores displaced with different concentrations of nanoemulsions.

Compared to water displacement, nanoemulsion shows greater efficiency in displacing crude oil from macropores. Additionally, a more uniform decrease in the spectra is observed, which contrasts with the water displacement at different temperatures shown in Fig. 10. It is well known that under wax deposition conditions, the presence of waxy mixtures either reduces the flow channel size by adhering to the rock pore surfaces or exhibits elasticity and pronounced thixotropic behavior, both of which make fluid flow more difficult (Zhao et al., 2024). From Fig. 6, it can be seen that the addition of nanoemulsions can dissolve some of the precipitated wax crystals. The agglomeration structure of wax crystals gradually decomposes to become relatively dispersed and not cross-linked with each other, thus effectively improving the flow capacity of crude oil. This is conducive to the effective displacement of crude oil from the core by nanoemulsion, and the peak value and area of the spectrum decrease uniformly. The higher the concentration of nanoemulsion, the higher the displacement efficiency, although the replaced crude oil is still mainly from the macropores.

4.2.4. Crude oil recovery comparison

The recovery data under different displacement conditions are shown in Fig. 13. Thermal water displacement aligns with expectations, as thermal energy reduces crude oil viscosity, facilitates wax crystal dissolution. This improves crude oil mobility and minimizes wax deposition, and diminishes the ease of crude oil displacement, thereby increasing recovery. However, the contribution to improving recovery mainly comes from macropores. Taking low-permeability core samples as an example, when the displacement fluid temperature increases from 30 to 60 °C, the crude oil recovery in macropores rises from 15.30% to 24.80%, and the overall recovery increases from 19.36% to 32.82%.

Compared with the low-permeability core, the overall recovery of the high-permeability core is improved, and the oil recovery in the micropores is also increased significantly. It can be seen that as the permeability of the core increases, the flow capacity of the displacement fluid within the core also increases, enabling effective displacement of crude oil. As cores #5 and #6 were fractured along the longitudinal direction, the water has a favorable flow channel in the displacement direction, which is convenient for crude oil to be displaced. As shown in Fig. 13, the overall recovery of cores #5 and #6 is high, even in the case of wax deposition of crude oil at 30 °C. This is still because the presence of a fracture increases the contact area between water and the core, allowing the water to enter the interior of the core pores more conveniently and drive the crude oil in the pores out of the core. In addition, the longer the fracture extends along the core, the higher the recovery.

The addition of nanoemulsion reduced wax deposition by dissolving existing wax crystals, inhibiting the precipitation of new wax crystals, and ultimately leading to an increase in the oil

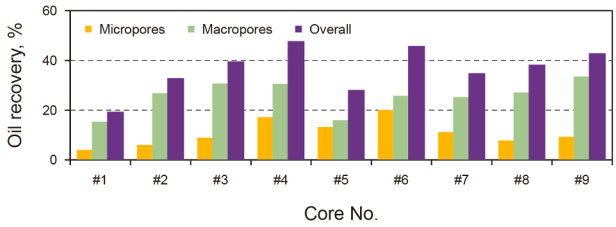

Fig. 13. Crude oil recovery data. #1 and #2 are 20 mD cores, #3 and #4 are 200 mD cores, and #5 and #6 are fractured cores, all of which were displaced with water. #7–#9 are 20 mD cores, which were displaced with nanoemulsions at concentrations of 0.1, 0.5, and 1.0 wt%, respectively. For cores #2 and #4, the displacement fluid temperatures were 60 °C; and the rest were 30 °C.

recovery. After adding 1 wt% nanoemulsion, the overall oil recovery is as high as 42.85%. At the same time, as the concentration of nanoemulsion increases, the change of crude oil recovery in core macropores is more obvious, which is similar to the effect of increasing the displacement fluid temperature. However, there are also differences between the two. By comparing the T_2 spectrum changes of the two, it can be seen that the spectrum decreases uniformly during nanoemulsion displacement, indicating that the nanoemulsion can continuously and effectively dissolve the wax crystals of crude oil in the pore space of the core and drive them out of the core, thereby achieving a higher recovery.

5. Discussion

5.1. Magnetic resonance imaging (MRI) evolution during core displacement

MRI can be used to monitor the distribution characteristics of crude oil in the core at different moments; the redder the color in MRI, the higher the oil content (Zhao G.-J. et al., 2023). Fig. 14 shows the displacement conditions for different cores and the images collected before and after displacement.

Firstly, comparing the scanned images of cores with low permeability before and after displacement at 30 °C, it can be seen

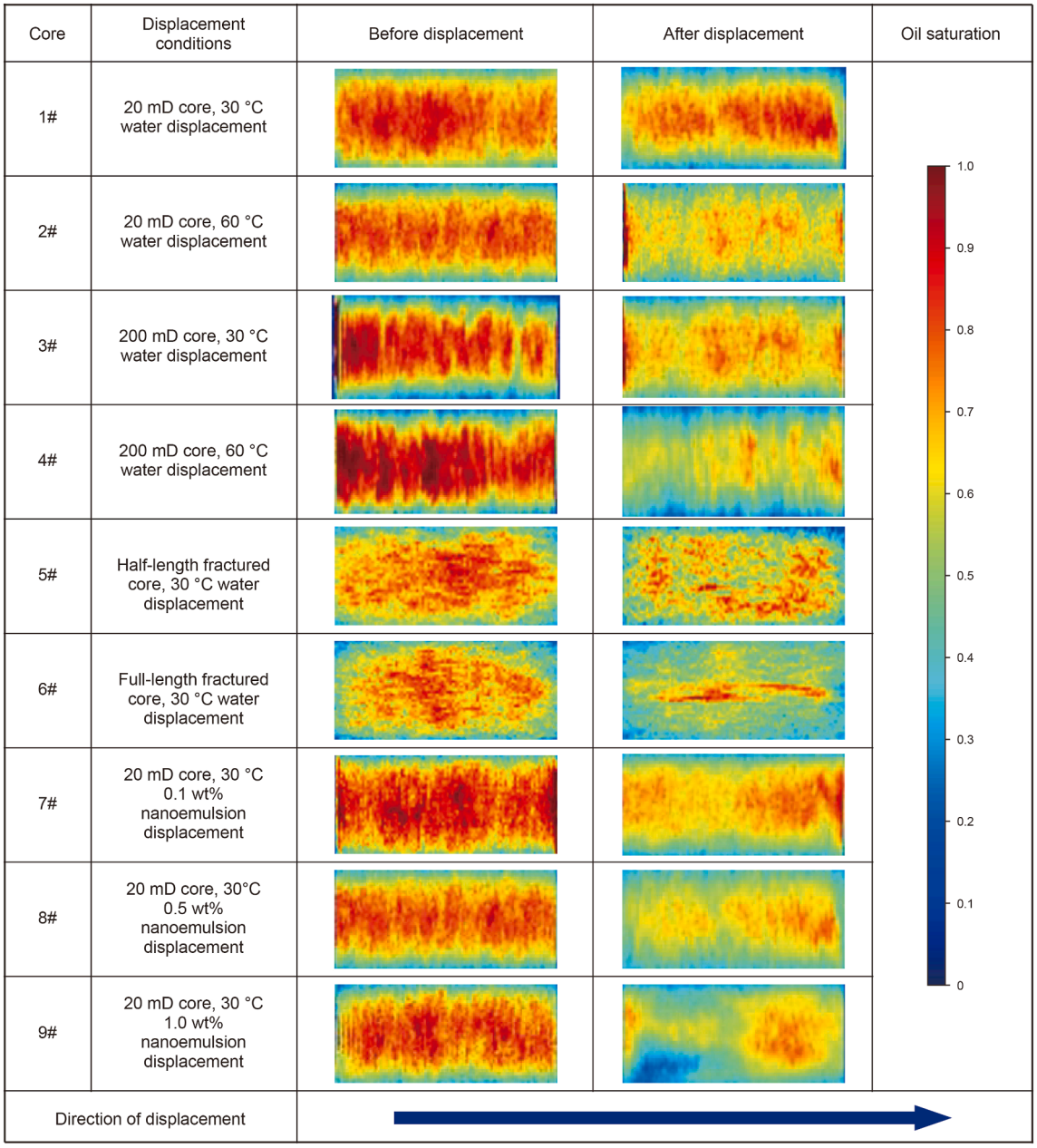

Fig. 14. MRI of different cores before and after displacement.

that a large area of deep red color remains, indicating that the crude oil in this area is basically unused, and a large area of residual oil exists inside the core. With the gradual solidification of wax crystal molecules as well as the formation of waxy gel structure, wax precipitation damage occurs inside the core of waxy crude oil (Bai and Zhang, 2013; Li et al., 2020), coupled with the uneven distribution of pore space or poor connectivity of seepage channels within the core, a large area of crude oil has not been effectively driven off (Kané et al., 2003). After hot water displacement, there is no large red area in the image, and the crude oil has been effectively displaced. Therefore, thermal recovery is particularly essential for highly waxy oilfields.

With the increase in core permeability or the existence of a fracture, water can more conveniently drive out the crude oil in the core pores, and thus the oil saturation is reduced from the MRI image after the displacement. In addition, by comparing MRI images before and after nanoemulsion displacement, it can be seen that the deep red area of the core becomes lighter after displacement, indicating a decrease in oil saturation. Moreover, as the concentration of nanoemulsion increases, the change becomes more obvious. This further demonstrates that nanoemulsion can effectively improve wax deposition damage in waxy crude oil, thereby increasing crude oil recovery.

5.2. Scanning electron microscope observation and interfacial tension data

Based on the results of the NMR core displacement experiment described above, we further used a Verios 5 XHR scanning electron microscope (SEM) and a BZY-2 interfacial tension meter to study the intrinsic mechanism of low recovery during low-temperature displacement and how nanoemulsion can improve the recovery of waxy crude oil. Fig. 15 shows the microscopic retention of crude oil on the core surface after displacement under different conditions, and Table 5 shows the interfacial tension data between different displacement fluids and crude oil.

At low temperatures, crude oil inside core pores predominantly adheres along the pore surfaces (Fig. 15(a)). In this state, the core exhibits strong oil-wet characteristics, and the precipitated wax within the crude oil forms a waxy gel structure. This structure exhibits pronounced elasticity and thixotropic behavior, even displaying quasi-solid properties, which significantly reduces the mobility of crude oil within the rock matrix, and there is wax deposition damage (Li X. et al., 2024; Trushin et al., 2021; Zhao et al., 2024). At this time, the injection of water into the core can only strip the crude oil that is not firmly attached or crush the larger crude oil and carry it outside the core. The remaining waxy crude oil trapped in the rock pores remains attached to the rock pore surface in small pieces (Fig. 15(b)), which explains the limited recovery from water displacement at low temperatures. When the displacement fluid temperature rises above the WAT, the structure of the gel in the waxy crude oil is destroyed. Most of the crude oil remaining in the pores with flow capacity will be expelled outside the core, and the rest of the crude oil that has not been expelled is mostly remaining oil attached to the pores and has lost its flow capacity (Xie et al., 2020).

Table 5
Interfacial tension between displacement fluids and crude oil.

Displacement fluid	Temperature, °C	Interfacial tension, mN/m
Water	30	48.32
Water	60	16.67
0.1 wt% nanoemulsion	30	25.26
0.5 wt% nanoemulsion	30	21.08
1.0 wt% nanoemulsion	30	12.22

The addition of nanoemulsion can reduce the oil–water interfacial tension (Table 5). The reason for this is that with the injection of nanoemulsion displacement agent, polyoxyethylene alcohol ether (surfactant) and low-carbon chain alcohol (cosurfactant) interact with each other, which reduces the oil–water interfacial tension and increases the contact area between oil and water, and waxy crude oil is easier to be stripped (Yuan et al., 2023). At the same time, the low interfacial tension makes the waxy crude oil more stable in the displacement agent, which is not easy to coalesce and will not increase the flow resistance, so that the waxy gel structure in the stripping state will not be further crosslinked, and the wax deposition damage will be reduced, which will help to further improve the recovery of crude oil in waxy reservoirs (He et al., 2016).

5.3. Analysis of wax deposition damage reduction and enhanced oil recovery mechanism

In summary, the primary objective for the further development of highly waxy crude oil reservoirs is to enhance reservoir crude oil seepage capacity while minimizing the adverse effects of wax deposition. Based on current experimental results, due to the wax deposition and viscosity increase of highly waxy crude oil at low temperature, crude oil flow is severely restricted. Cold water mainly relies on increasing the displacement pressure to drive the flowing crude oil out of the core, and its recovery is relatively limited (Fig. 16(b)). In contrast, thermal water displacement utilizes heat to reduce crude oil viscosity and dissolve wax crystals, thereby improving crude oil mobility. Higher temperatures reduce wax deposition and weaken the stability of the gel structure, making crude oil displacement easier (Xie et al., 2020). However, based on NMR displacement experiments, its EOR growth is

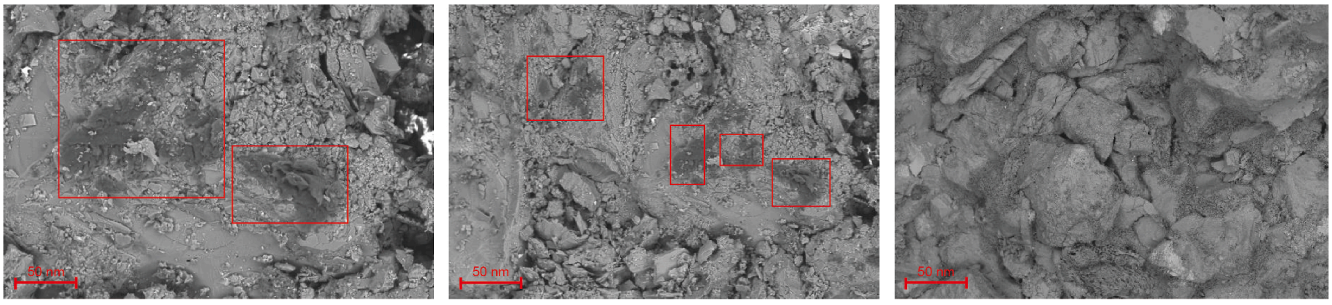

(a) Before displacement **(b)** After water displacement **(c)** After nanoemulsion displacement

Fig. 15. SEM images before and after displacement.

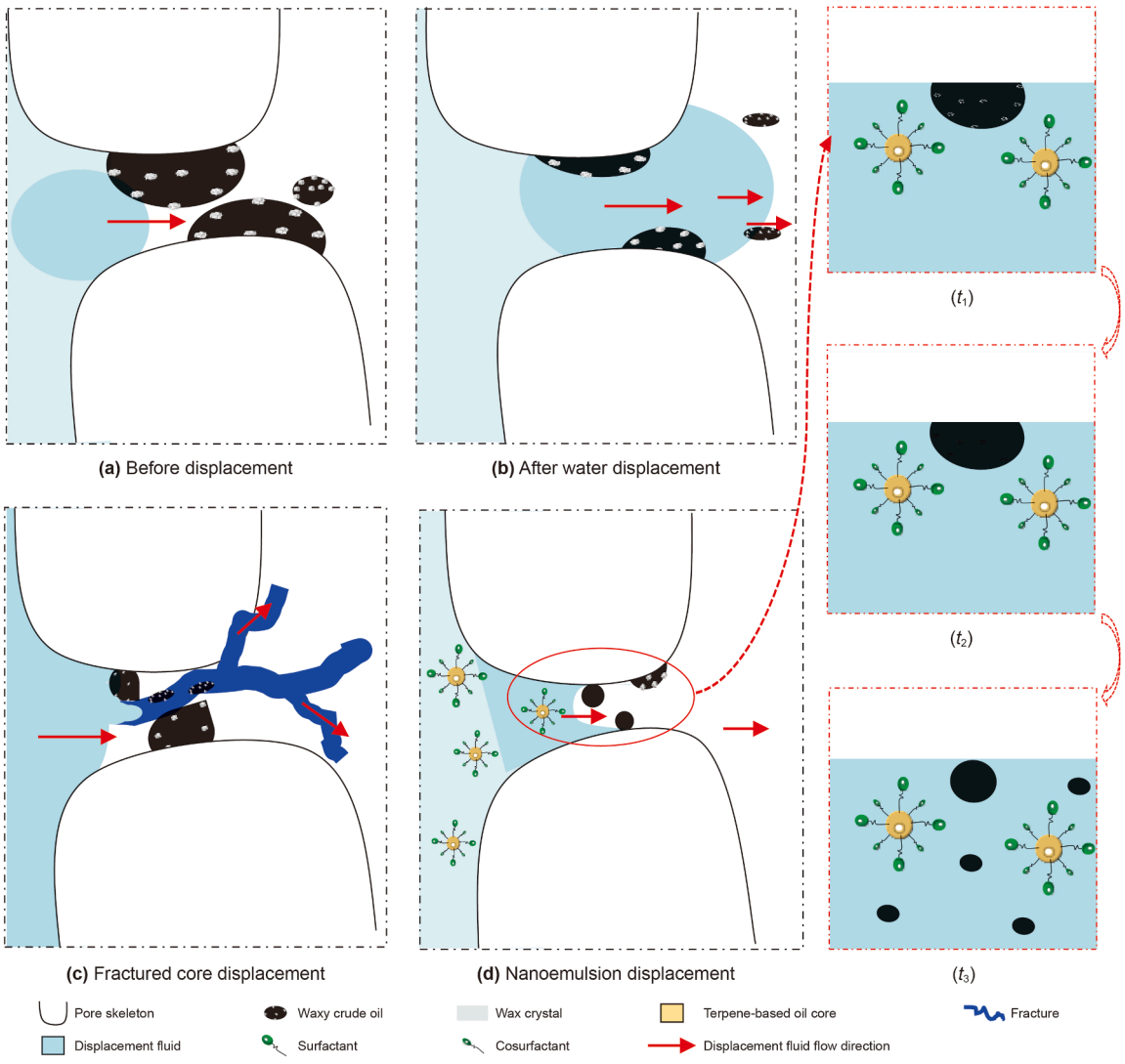

Fig. 16. Mechanisms for enhancing oil recovery under different displacement conditions (t_1 to t_3 are the different moments from the dissolution of wax crystals by nanoemulsion to the reduction of interfacial tension and then to the displacement of waxy crude oil outside the core).

limited compared to other recovery measures. By increasing the permeability of the core or creating fractures in the core through fracturing technology, the flowability of the displacement fluid within the core can be improved, facilitating the displacement of flowable crude oil within the core pores. At the same time, the fractures can increase the contact area between the displacement fluid and the core, facilitating the entry of the displacement fluid into the core pores and alleviating wax deposition damage (Fig. 16(c)). In addition, these two methods can effectively improve the recovery of crude oil in the micropores of the core.

In low-permeability reservoirs, the nanoemulsion primarily enhances oil recovery by reducing oil–water interfacial tension, facilitating the detachment of crude oil from pore surfaces (Yuan et al., 2023) (Fig. 16(d), at montents t_1–t_3). Additionally, the nanoemulsion induces a wettability reversal, altering initially oil-wet rock surfaces to water-wet conditions. This modification enhances the mobility of the displacing fluid within the interconnected porous medium, thereby promoting the detachment of waxy crude oil from rock surfaces, mitigating wax deposition damage, and improving crude oil recovery (Li X. et al., 2024; Wang et al., 2024). Furthermore, the terpenoid components in the nanoemulsion, serving as primary wax-dissolving agents, share structural and physicochemical similarities with wax crystal molecules. This enables them to dissolve precipitated wax crystal aggregates and inhibit the formation of waxy gel structures, effectively lowering the WAT and wax deposition damage of crude oil and reducing the viscoelasticity of highly waxy crude oil, thereby enhancing its mobility and final recovery (Ding et al., 2023; El Naggar et al., 2016; Yao et al., 2016).

6. Conclusions

This paper comprehensively studies the damage characteristics of wax deposition in low-permeability and waxy oil reservoirs and investigates EOR of waxy crude oil under different water displacement temperatures, fractured-core conditions, and nanoemulsion concentrations. The main conclusions are as follows:

(1) Waxy crude oil is affected by wax deposition and waxy gel structure, resulting in wax deposition damage. At 30 °C, the overall recovery is only 19.36%. After injecting 60 °C hot water, the recovery can be increased to 32.82%, which can alleviate wax deposition damage to a certain extent.

(2) Improving core permeability or fractured core can improve the flow capacity of displacement fluid in the core, thereby alleviating wax deposition damage of waxy crude oil and improving recovery. Meanwhile, this method effectively improves EOR in a micropore core.
(3) The addition of nanoemulsion decreases the number, area ratio, average aspect ratio, and fractal dimension of wax crystals, resulting in simpler crystal morphology. Using a 1 wt% of nanoemulsion, the area ratio of wax crystals decreased from 47.25% to 16.67%, and the number of wax crystals decreased from 1309 to 496.
(4) Nanoemulsions can dissolve wax crystals, inhibit their formation, and reduce oil–water interfacial tension, thereby mitigating wax deposition damage and improving the recovery of waxy crude oil. Using nanoemulsions with concentrations of 0.1, 0.5, and 1.0 wt%, the overall crude oil recovery reached 34.84%, 38.24%, and 42.85%, respectively.

CRediT authorship contribution statement

Rui-Jie Fei: Writing – review & editing, Writing – original draft, Validation, Resources, Methodology, Data curation. **Ming-Hui Li:** Methodology, Conceptualization, Writing – review & editing. **Shuai Yuan:** Visualization, Validation, Investigation. **Chen Cao:** Software, Formal analysis. **Fu-Jian Zhou:** Resources, Project administration, Funding acquisition. **Er-Dong Yao:** Resources, Funding acquisition. **Hao Bai:** Supervision, Data curation. **Diu-Wei Ding:** Resources, Funding acquisition.

Data availability

Data will be made available on request.

Declaration of competing interest

The authors declare that they have no known competing financial interests or personal relationships that could have appeared to influence the work reported in this paper.

Acknowledgements

This study is supported by the National Science and Technology Major Project (2017ZX05009-005-003) and the National Natural Science Foundation of China (U23B2084).

References

Adebiyi, F.M., 2020. Paraffin wax precipitation/deposition and mitigating measures in oil and gas industry: A review. Petrol. Sci. Technol. 38 (21), 962–971. https://doi.org/10.1080/10916466.2020.1804400.
Ali, S.I., Lalji, S.M., Haneef, J., Khan, M.A., Yousufi, M., Yousaf, N., et al., 2022. Phenomena, factors of wax deposition and its management strategies. Arabian J. Geosci. 15 (2), 133. https://doi.org/10.1007/s12517-021-09221-6.
Al-Shboul, T.S., Sagala, F., Nassar, N., 2023. Role of surfactants, polymers, nanoparticles, and its combination in inhibition of wax deposition and precipitation: A review. Adv. Colloid Interface Sci. 315, 102904. https://doi.org/10.1016/j.cis.2023.102904.
Babadagli, T., 2003. Evaluation of EOR methods for heavy-oil recovery in naturally fractured reservoirs. J. Pet. Sci. Eng. 37 (1), 25–37. https://doi.org/10.1016/S0920-4105(02)00309-1.
Bai, C., Zhang, J., 2013. Thermal, macroscopic, and microscopic characteristics of wax deposits in field pipelines. Energy Fuels 27 (2), 752–759. https://doi.org/10.1021/ef3017877.
Benavides, F., Leiderman, R., Souza, A., Carneiro, G., Bagueira de Vasconcellos Azeredo, R., 2020. Pore size distribution from NMR and image based methods: A comparative study. J. Pet. Sci. Eng. 184, 106321. https://doi.org/10.1016/j.petrol.2019.106321.
Burger, E.D., Perkins, T.K., Striegler, J.H., 1981. Studies of wax deposition in the trans Alaska pipeline. J. Petrol. Technol. 33 (6), 1075–1086. https://doi.org/10.2118/8788-PA.
Cao, J., Liu, L., Liu, C., He, C., 2022a. Phase transition mechanisms of paraffin in waxy crude oil in the absence and presence of pour point depressant. J. Mol. Liq. 345, 116989. https://doi.org/10.1016/j.molliq.2021.116989.
Cao, L., Sun, J., Liu, J., Liu, J., 2022b. Experiment and application of wax deposition in Dabei deep condensate gas wells with high pressure. Energies 15 (17), 6200. https://doi.org/10.3390/en15176200.
Chen, J., Deng, C., Wang, X., Ni, Y., Sun, Y., Zhao, Z., et al., 2017. Formation mechanism of condensates, waxy and heavy oils in the southern margin of Junggar Basin, NW China. Sci. China Earth Sci. 60 (5), 972–991. https://doi.org/10.1007/s11430-016-9027-3.
Ding, J., Zhang, J., Li, H., Zhang, F., Yang, X., 2006. Flow behavior of daqing waxy crude oil under simulated pipelining conditions. Energy & Fuels 20 (6), 2531–2536. https://doi.org/10.1021/ef060153t.
Ding, X., Li, B., Xu, T., Feng, L., 2023. Efficient and environmentally friendly chemical dewaxing and anti-waxing technology and its application in waxed oil wells. Spec Petrochem 40 (2), 23–264 (in Chinese).
Dong, H., Zhao, J., Wei, L., Liu, Y., Li, Y., 2020. Effect of initial cooling temperature on structural behaviors of gelled waxy crude oil and microscopic mechanism investigation. Energy & Fuels 34 (12), 15782–157801. https://doi.org/10.1021/acs.energyfuels.0c02274.
Eke, W.I., Ituen, E., Yuanhua, L., Akaranta, O., 2022. Laboratory evaluation of modified cashew nut shell liquid as oilfield wax inhibitors and flow improvers for waxy crude oils. Upstream Oil Gas Technol. 8, 100068. https://doi.org/10.1016/j.upstre.2022.100068.
El Naggar, A.M.A., Mostafa, M.S., Zaky, M.T., 2016. New trend for the pour point depression of a waxy petroleum fraction with in-situ desulphurization using (O_2H & OH) radicals coupled with nanoparticles of titanium compounds. Fuel 180, 218–227. https://doi.org/10.1016/j.fuel.2016.04.031.
El-Dalatony, M., Jeon, B.-H., Salama, E.-S., Eraky, M., Kim, W.B., Wang, J., et al., 2019. Occurrence and characterization of paraffin wax formed in developing wells and pipelines. Energies 12 (6), 967. https://doi.org/10.3390/en12060967.
Elsayed, M., Isah, A., Hiba, M., Hassan, A., Al-Garadi, K., Mahmoud, M., et al., 2022. A review on the applications of nuclear magnetic resonance (NMR) in the oil and gas industry: Laboratory and field-scale measurements. J. Pet. Explor. Prod. Technol. 12 (10), 2747–2784. https://doi.org/10.1007/s13202-022-01476-3.
Gurgel Aum, Y.K.P., Aum, P.T.P., Silva, D.N.N., Braga, N.P., Souza, C.D.R., Barros Neto, E.L., Dantas, T.N.C., 2024. Effective removal of paraffin deposits using oil-in-water microemulsion systems. Fuel 358 (Part A), 130112. https://doi.org/10.1016/j.fuel.2023.130112.
He, C., Ding, Y., Chen, J., Wang, F., Gao, C., Zhang, S., et al., 2016. Influence of the nano-hybrid pour point depressant on flow properties of waxy crude oil. Fuel 167, 40–48. https://doi.org/10.1016/j.fuel.2015.11.031.
Huang, Z., Lu, Y., Hoffmann, R., Amundsen, L., Fogler, H.S., 2011. The effect of operating temperatures on wax deposition. Energy & Fuels 25 (11), 5180–5188. https://doi.org/10.1021/ef201048w.
Japper-Jaafar, A., Bhaskoro, P.T., Mior, Z.S., 2016. A new perspective on the measurements of wax appearance temperature: Comparison between DSC, thermomicroscopy and rheometry and the cooling rate effects. J. Pet. Sci. Eng. 147, 672–681. https://doi.org/10.1016/j.petrol.2016.09.041.
Kané, M., Djabourov, M., Volle, J.-L., Lechaire, J.-P., Frebourg, G., 2003. Morphology of paraffin crystals in waxy crude oils cooled in quiescent conditions and under flow. Fuel 82 (2), 127–135. https://doi.org/10.1016/S0016-2361(02)00222-3.
Kané, M., Djabourov, M., Volle, J.-L., 2004. Rheology and structure of waxy crude oils in quiescent and under shearing conditions. Fuel 83 (11), 1591–1605. https://doi.org/10.1016/j.fuel.2004.01.017.
Kasumu, A.S., Arumugam, S., Mehrotra, A.K., 2013. Effect of cooling rate on the wax precipitation temperature of “waxy” mixtures. Fuel 103, 1144–1147. https://doi.org/10.1016/j.fuel.2012.09.036.
Kiyingi, W., Guo, J.-X., Xiong, R.-Y., Su, L., Yang, X.-H., Zhang, S.-L., 2022. Crude oil wax: A review on formation, experimentation, prediction, and remediation techniques. Pet. Sci. 19 (5), 2343–2357. https://doi.org/10.1016/j.petsci.2022.08.008.
Li, B., Guo, Z., Zheng, L., Shi, E., Qi, B., 2024. A comprehensive review of wax deposition in crude oil systems: Mechanisms, influencing factors, prediction and inhibition techniques. Fuel 357, 129676. https://doi.org/10.1016/j.fuel.2023.129676.
Li, H., Zhang, J., Xu, Q., Hou, C., Sun, Y., Zhuang, Y., et al., 2020. Influence of asphaltene on wax deposition: Deposition inhibition and sloughing. Fuel 266, 117047. https://doi.org/10.1016/j.fuel.2020.117047.
Li, M., Chen, X., Wang, Q., Diao, D., Zhang, Y., Wang, C., et al., 2024. Studying the effects of asphaltene oxidation on wax crystallization and rheological properties in waxy crude oils. Fuel 362, 130767. https://doi.org/10.1016/j.fuel.2023.130767.
Li, X., Zhao, L., Fei, R., Wang, J., Liu, S., Li, M., et al., 2024. Cooling damage characterization and chemical-enhanced oil recovery in low-permeable and high-waxy oil reservoirs. Processes 12 (2), 421. https://doi.org/10.3390/pr12020421.
Macary, S., Mahtumov, N., Muhamadiyev, H., Akyyev, A., Mashadov, G., Al-Hassan, A., et al., 2018. Wax management: Comprehensive approach to assure flow in harsh climate-brown field conditions. In: SPE Russian Petroleum Technology Conference. https://doi.org/10.2118/191541-18RPTC-MS.

Nie, X., Yang, S., 2014. Numerical simulation of paraffin wax deposition in waxy crude oil reservoir with cold water flooding. Geosystem Eng. 17 (4), 219–225. https://doi.org/10.1080/12269328.2014.959623.
Ragunathan, T., Husin, H., Wood, C.D., 2020. Wax formation mechanisms, wax chemical inhibitors and factors affecting chemical inhibition. Appl. Sci. 10 (2), 479. https://doi.org/10.3390/app10020479.
Sun, Z., Li, M., Yuan, S., Zhou, F., Fei, R., 2023. The effect of the fracture geometries from different stratification angle on the imbibition recovery of Jimusar shale oil: A comprehensive experimental study. Geoenergy Sci. Eng. 229, 212067. https://doi.org/10.1016/j.geoen.2023.212067.
Sun, Z., Li, M., Yuan, S., Hou, X., Bai, H., Zhou, F., et al., 2024. The flooding mechanism and oil recovery of nanoemulsion on the fractured/non-fractured tight sandstone based on online LF-NMR experiments. Energy 291, 130226. https://doi.org/10.1016/j.energy.2023.130226.
Temizel, C., Canbaz, C.H., Tran, M., Abdelfatah, E., Jia, B., Putra, D., et al., 2018. A comprehensive review: Heavy oil reservoirs, latest techniques, discoveries, technologies and applications in the oil and gas industry. In: SPE International Conference and Exhibition on Formation Damage Control. https://doi.org/10.2118/193646-MS.
Towler, B.F., Jaripatke, O., Mokhatab, S., 2011. Experimental investigations of the mitigation of paraffin wax deposition in crude oil using chemical additives. Petrol. Sci. Technol. 29 (5), 468–483. https://doi.org/10.1080/10916460903394029.
Trushin, Y.M., Aleshchenko, A.S., Zoshchenko, O.N., Arsamakov, M.S., Tkachev, I.V., Kruglov, D.S., 2021. A new approach to simulation of wax precipitation during cold water injection in carbonate reservoir of Kharyaga oilfield. In: SPE Russian Petroleum Technology Conference. https://doi.org/10.2118/206495-MS.
Vieira, L.C., Buchuid, M.B., Lucas, E.F., 2010. Effect of pressure on the crystallization of crude oil waxes. II. Evaluation of crude oils and condensate. Energy & Fuels 24 (4), 2213–2220. https://doi.org/10.1021/ef900761t.
Wang, H., Boyer, S.A.E., Bellet, M., Dalle, F., 2023. Effects of wax components and the cooling rate on crystal morphology and mechanical properties of wax–oil mixtures. Cryst. Growth Des. 23 (3), 1422–1433. https://doi.org/10.1021/acs.cgd.2c00941.
Wang, L., He, Y., Chen, H., Meng, Z., Wang, Z., 2019. Experimental investigation of the live oil-water relative permeability and displacement efficiency on Kingfisher waxy oil reservoir. J. Pet. Sci. Eng. 178, 1029–1043. https://doi.org/10.1021/acs.cgd.2c00941.
Wang, M., Yang, S., Zheng, Z., Yu, T., Yang, C., Guo, F., 2020. Study and analysis of methods for determining wax evolution temperature. J. Petrochem. Univ. 33 (4), 43–48. https://doi.org/10.3969/j.issn.1006-396X.2020.04.008 (in Chinese).
Wang, M., Yang, S., Li, J., Zheng, Z., Wen, J., Ma, Q., et al., 2021. Cold water-flooding in a heterogeneous high-pour-point oil reservoir using computerized tomography scanning: Characteristics of flow channel and trapped oil distribution. J. Pet. Sci. Eng. 202, 108594. https://doi.org/10.1016/j.petrol.2021.108594.
Wang, Q., Zhou, F., Su, H., Zhang, S., Dong, R., Yang, D., et al., 2024. Experimental evaluations of nano high-viscosity friction reducers to improve acid fracturing efficiency in low-permeability carbonate reservoirs. Chem. Eng. J. 483, 149358. https://doi.org/10.1016/j.cej.2024.149358.
Xia, X., Li, C., Dai, S., Duan, Z., Lian, W., Yao, B., et al., 2022. Modification effect of macroporous comb-like polymeric pour point depressants on the flow behavior of model waxy oils. Fuel 314, 123113. https://doi.org/10.1016/j.fuel.2021.123113.
Xie, J., Hu, X., Liang, H., Wang, M., Guo, F., Zhang, S., et al., 2020. Cold damage from wax deposition in a shallow, low-temperature, and high-wax reservoir in Changchunling Oilfield. Sci. Rep. 10 (1), 14223. https://doi.org/10.1038/s41598-020-71065-z.
Yalaoui, I., Chevalier, T., Levitz, P., Darbouret, M., Palermo, T., Vinay, G., et al., 2020. Probing multiscale structure and dynamics of waxy crude oil by low-field NMR, X-ray scattering, and optical microscopy. Energy & Fuels 34 (10), 12429–12439. https://doi.org/10.1021/acs.energyfuels.0c02453.
Yan, D., Luo, Z., 1987. Rheological properties of Daqing crude oil and their application in pipeline transportation. SPE Prod. Eng. 2 (4), 267–276. https://doi.org/10.2118/14854-PA.
Yang, J., Lu, Y., Daraboina, N., Sarica, C., 2020. Wax deposition mechanisms: Is the current description sufficient? Fuel 275, 117937. https://doi.org/10.1016/j.fuel.2020.117937.
Yang, S.L., Wu, X.H., Wang, Y.X., Yang, X.Y., Chen, H., Li, L.C., et al., 2013. Wax deposition in pores and the permeability change for high-wax crude in a sandstone reservoir. Petrol. Sci. Technol. 31 (18), 1891–1898. https://doi.org/10.1080/10916466.2011.588642.
Yao, B., Li, C., Yang, F., Zhang, Y., Xiao, Z., Sun, G., 2016. Structural properties of gelled changqing waxy crude oil benefitted with nanocomposite pour point depressant. Fuel 184, 544–554. https://doi.org/10.1016/j.fuel.2016.07.056.
Yuan, S., Zhou, F., Li, Y., Sheng, L., Liang, T., Tang, X., et al., 2023. A comprehensive study on the enhancements of rheological property and application performances for high viscous drag reducer by adding diluted microemulsion. Geoenergy Sci. Eng. 227, 211770. https://doi.org/10.1016/j.geoen.2023.211770.
Zhang, H., Zhao, Y., Chen, X., Dong, L., Yu, H., Deng, J., et al., 2024. Effect of a novel type of water-in-oil nanocomposite viscosity improver on rheological properties of crude oil. Petrol. Sci. Technol. 42 (24), 3563–3579. https://doi.org/10.1080/10916466.2023.2208602.
Zhang, J., Guo, L., Gao, X., Shi, C., 2025. Microscopic mechanism of wax precipitation and gelation of waxy crude oil based on molecular dynamics simulation. J. Pipeline Sci. Eng., 100311 https://doi.org/10.1016/j.jpse.2025.100311.
Zhang, Y., Gai, C., Song, B., Jiang, J., Wang, Z., 2023. The influence of permeability and heterogeneity on chemical flooding efficiency and remaining oil distribution—based on NMR displacement imaging. Sci. Rep. 13 (1), 14316. https://doi.org/10.1038/s41598-023-39535-2.
Zhao, G.-J., Yang, M.-J., Lv, X., Zheng, J.-N., Song, Y.-C., 2023. MRI insight on multiphase flow in hydrate-bearing sediment and development mechanism of hydrate seal. Pet. Sci. 20 (6), 3854–3864. https://doi.org/10.1016/j.petsci.2023.07.017.
Zhao, J., Xi, X., Dong, H., Wang, Z., Zhuo, Z., 2022. Rheo-microscopy in situ synchronous measurement of shearing thinning behaviors of waxy crude oil. Fuel 323, 124427. https://doi.org/10.1016/j.fuel.2022.124427.
Zhao, J., Li, X.-F., Dong, H., Wang, Z.-H., 2023. Rheo-optic in situ synchronous study on the gelation behaviour and mechanism of waxy crude oil emulsions. Pet. Sci. 20 (2), 1266–1288. https://doi.org/10.1016/j.petsci.2022.08.033.
Zhao, J., Zhuo, Z., Dong, H., Wang, Z., 2024. Structural failure process of gelled waxy crude oil emulsion based on rheological-in-situ microscopic synchronous measurement. Fuel 364, 131070. https://doi.org/10.1016/j.fuel.2024.131070.
Zhou, W., Tang, Z., Orodu, O.D., 2010. Case study of the impact of cold and hot waterflooding performance by simulation and experiment of high pour point oil reservoir, Liaohe Oilfield, North-East China. In: SPE Oil and Gas India Conference and Exhibition. https://doi.org/10.2118/128873-MS.